

# Face Reenactment via Generative Landmark Guidance

Chen Hu, Xianghua Xie\*, Lin Wu

Department of Computer Science, Swansea University, UK

\*x.xie@swansea.ac.uk

**Abstract**—The identity preserving problem is one of the major obstacles in face reenactment. The problem occurs when the model fails to preserve the detailed information of the source identity, and especially obvious when reenacting different identities. The underlying factors may include the leaking of driver identity, due to the identity mismatch, and unseen large head poses. In this paper, we propose a novel face reenactment approach via generative landmark coordinates. Specifically, a conditional generative adversarial network is developed to estimate reenacted landmark coordinates for the driving image, which successfully excludes its identity information. These generated coordinates are further injected into the subsequent inference style transfer module to increase the realism of face images. We evaluated our method on the VoxCeleb1 dataset for self-reenactment and the CelebV dataset for reenacting different identities. Extensive experiments demonstrate that our method can produce more realistic reenacted face images.

**Index Terms**—face reenactment, GAN, style transfer, facial landmarks

## I. INTRODUCTION

Face reenactment is a conditional image generation task. The input, namely the condition, to a face reenactment model comprises two parts, the source and the driving. The source is one or a set of images of a specific person, serving to provide appearance features of the person. The driving image is another image with an arbitrary face. The goal of face reenactment is to transfer the head pose and expression from the driving image to the face in the source image. Real world application of face reenactment includes video conferencing and film production. In the scenario video conferencing, the speaker’s face can be reenacted to match the face motion of a translator [1]. In film industry, face reenactment can be used in a similar fashion, creating more natural localized motion pictures in different languages. Film makers can also fine-tune actors’ facial movements with the help of face reenactment models.

Given the fact that it is infeasible to collect image pairs of two different people with identical head pose and expression, the self-supervised training strategy proposed by authors of X2Face [6] greatly helped the evolution of face reenactment methods. During training, the self-supervised strategy constrains the source and driving image in an input pair to be taken from the same video clip of the same person, therefore the driving image is also the groundtruth for the generated image. Despite the ease of training, in the testing scenario where the source and driving image are taken from different people, models trained by this strategy is at the risk of mixing

the driving’s identity in the image generator, resulting in the identity preserving problem, that is, the reenacted image shares structural similarity with both people in the input, instead of being the exact person in the source image.

Location of facial landmarks is valuable for defining a person’s identity and head pose. During self-supervised training, if the eyes, nose and mouth in the generated image are precisely aligned with their corresponding location in the driving image, the generated image is more likely to be a faithful reenactment. Landmark locations can then be used to guide the model in the self-reenactment scenario. However, when reenacting different people, landmark locations in the driving image do not lead to desired output, as the locations now reflects the facial structures of different people, which can only aggravate the identity preserving problem. To help face reenactment methods benefit from landmark location, landmark coordinates also need to be reenacted. If these coordinates reflect the source’s identity while matching the driving’s head pose and expression, they can guide the model to process the test sample as if it is a self-reenactment case.

To obtain more realistic landmark estimation, we model this problem from the perspective of face reenactment evaluation. Specifically, for a generated face to be considered as a good reenactment, the generated face should look like the same person in the source image. Meanwhile, the generated pose and expression should match the ones in the driving image. We then propose a conditional generative adversarial network (GAN) to generate facial landmark points based on a person’s identity as well as the desired head pose and expression. We follow the convention of face reenactment evaluation to formulate the head pose as pitch, yaw and roll angles, the expressions are formulated as the combination of facial action units (AUs) [16], which are considered the fundamental components of human face expressions. The proposed landmark GAN is not only beneficial for improving the performance, but it may also be employed to semantically generate human faces with expressions. This is because expressions can be decomposed into combinations of AUs. Given a combination of AUs, our landmark GAN can estimate fiducial points that match the desired expression, which can be subsequently used to generate face images [38].

With generated landmark coordinates, we explicitly leverages them to guide the reenactment process. We align individual facial landmarks based on these coordinates, we also generate facial landmark heatmaps to yield style transfer

93 parameters, which are used to improve the realism of generated  
94 faces. Our contributions of this paper can be summarized  
95 below:

96 1) We propose a face reenactment method explicitly guided  
97 by facial landmark coordinates. An optical flow is first esti-  
98 mated based on the input source and driving image. The optical  
99 flow is a grid of coordinates determining where each pixel in  
100 the input should be moved into. We use the estimated optical  
101 flow to warp the feature maps of the source image. Individual  
102 landmarks are then respectively reenacted and aligned to guide  
103 the warped result.

104 2) We introduce a conditional landmark GAN that gener-  
105 ates landmark coordinates based on the input face’s identity,  
106 desired head pose angles and facial action units. In addition,  
107 we estimate style transfer parameters based on our estimated  
108 landmark coordinates to obtain more realist images. No in-  
109 formation on the driving’s identity is involved in these two  
110 modules.

111 3) We evaluate our method on the VoxCeleb1 [34] dataset  
112 for self-reenactment and the CelebV [35] dataset for reenacting  
113 different identities.

## 114 II. RELATED WORKS

### 115 A. Face Reenactment

116 Approaches to face reenactment can be categorized by the  
117 operation they used to generate new images, specifically, early  
118 face reenactment studies [1]–[5] mainly focus on rendering  
119 desired images from estimated 3D face models, while recent  
120 research more relies on optical flows to warp input images. The  
121 pipeline of rendering-based methods generally involves fitting  
122 3D faces from images, then morphing these 3D models and  
123 rendering the reenacted results. These methods often require a  
124 large quantity of video frames as inputs to extract texture fea-  
125 tures for rendering, they are also limited to reenacting specific  
126 people due to the availability of 3D models. Recent works [6]–  
127 [12] propose warping-based face reenactment methods which  
128 utilise optical flows to map pixels from the source image to  
129 the reenacted image. Image warping on convolutional neural  
130 networks (CNN) was first proposed in [13], where the model  
131 can estimate optical flows that warp skewed numerical digits  
132 back to the regular view, thus improving the classification  
133 accuracy. In the context of face reenactment, optical flows  
134 are estimated based on input images. Optical flows are used  
135 to warp the source images [6] or the feature maps of source  
136 images [7]–[9], [11]. Given an input image and an optical flow,  
137 the warping operation generates a new image by moving each  
138 pixel from the input image to the coordinate in the new image  
139 indicated by the optical flow.

140 As mentioned in Section I, obtaining images for different  
141 people with the exact same poses and expressions is infeasible  
142 in practice, a now widely adopted self-supervised learning  
143 paradigm was proposed in [6]. Given a source image sampled  
144 from a video sequence, a corresponding driving image of the  
145 same person is also randomly sampled from the same video,  
146 making supervised learning possible as the driving image is the

147 expected reenactment result. The self-supervised strategy sub-  
148 sequently leads to the identity preserving problem described  
149 in [7]. To remedy this issue, facial landmark coordinates are  
150 widely used as the guidance in face reenactment. The authors  
151 of ReenactGAN [35] built person-specific models to estimate  
152 landmark boundaries of reenacted faces. This method is ca-  
153 pable of predicting reasonable facial structure, however, it is  
154 required to train separate landmark boundary estimator for dif-  
155 ferent faces. MeshGCN [11] employed 3D Morphable Models  
156 (3DMM) to estimate dense 3D points on the reenacted faces.  
157 The work of [11] explicitly excludes the identity information  
158 of driving images by constructing reenacted 3D faces using  
159 the identity parameters of the source. This method achieved  
160 good performance in identity preserving. However, its optical  
161 flow estimation module is rather computationally heavy, as it  
162 is a graph convolutional neural network [15] that runs on the  
163 source and the reenacted meshes each with 53,215 vertices.  
164 Inspired by 3DMM, authors of [7] proposed a landmark  
165 transformer, which breaks down sparse 3D facial landmark  
166 coordinates into a base 3D face, and principal components that  
167 controls face shapes and expressions. This method was also  
168 later used by authors of [10]. By estimating corresponding  
169 principal component coefficients, the landmark transformer  
170 modifies landmark coordinates of the driving image to be  
171 more fitting to the identity of the source image. However, the  
172 performance of [7] is limited by the expressiveness of chosen  
173 principal components. The authors FSGANv2 [37] took an  
174 iterative approach to gradually rotate landmark coordinates  
175 through multiple steps until 2D landmark points match the  
176 desired poses. For the reenactment on expressions, FSGANv2  
177 directly swaps the mouth points in the source image with  
178 corresponding points from the driving image.

179 Compared to previous works, our method estimates sparse  
180 2D landmark coordinates in an end-to-end fashion through  
181 the landmark conditional GAN. The proposed method directly  
182 generates landmark points by considering the source’s identity,  
183 desired head pose angles and expressions. Similar to 3DMM,  
184 landmark points estimated by our method exclude the driving’s  
185 identity by only considering the source’s facial structure, but  
186 2D landmark points are more accessible than dense face  
187 vertices. In addition, our method adopts facial action units to  
188 formulate expressions instead of approximating by principal  
189 components. Evaluation results show that the proposed land-  
190 mark GAN helps our model greatly improve the performance  
191 on identity preserving while maintaining a relatively low head  
192 pose error.

### 193 B. Generative Adversarial Network

194 Generative adversarial networks (GANs) [17] are a family  
195 of neural networks that learn to map input from certain  
196 distribution to a desired distribution. A GAN consists of a  
197 generator and a discriminator, these two networks play a zero-  
198 sum game such that when the training converges, the discrim-  
199 inator can no longer differentiate generated samples from real  
200 ones, namely the generator learns to produce realistic data  
201 samples. The input to the generator is not limited to random

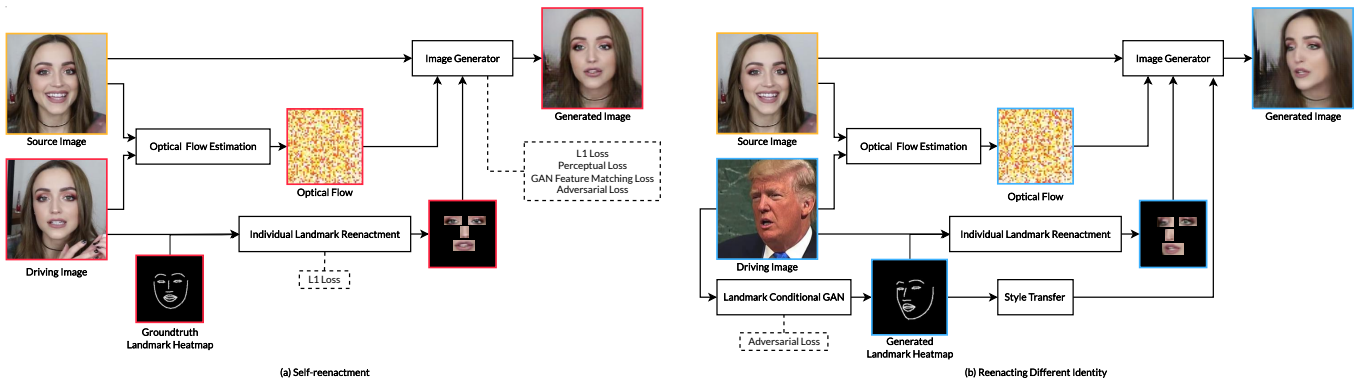


Fig. 1. Overview of proposed method for self-reenactment and reenacting different identities. Dashed boxes show loss functions that are responsible for the corresponding module.

202 variables sampled from a specified distribution, it can also be  
 203 categorical labels [18], texts [19] or even images [20], granting  
 204 more control over generated content. Face reenactment shares  
 205 similarity with the image-to-image translation, a generative  
 206 task that transfers an image from one domain to an image  
 207 in another domain. Authors of Pix2Pix [20] have shown that  
 208 supervision on pixel values combined with the use of GAN  
 209 yields most realistic image-to-image translation results. This  
 210 finding inspired many works on face reenactment, and GAN  
 211 has become an indispensable component when generating  
 212 realistic face images.

213 Vid2Vid [21] extended the work of Pix2Pix to generate  
 214 video frames. For the pipeline of Vid2Vid, past frames and  
 215 semantic segmentation maps are fed into the generator, an opti-  
 216 cal flow is estimated from the input and then applied to a past  
 217 frame to generate the video frame for the current time step.  
 218 The discriminator is responsible for the realness of generated  
 219 video frames while generated frames are also supervised by  
 220 the pixel values of real frames. Generative models such as  
 221 Pix2Pix and Vid2Vid are supervised by groundtruth examples,  
 222 and their input is also not non-stochastic, namely the input  
 223 domain and the output domain are both well-defined, therefore  
 224 these methods seldom consider the feature disentanglement  
 225 problem presents in models with stochastic nature. Pipelines of  
 226 optical flow based face reenactment methods are comparable  
 227 to that of Vid2Vid, optical flows are estimated from the source  
 228 and driving images, and then applied to the source image to  
 229 synthesize reenacted faces. In terms of the use of GAN to  
 230 generate face images, our method is also not an exception.  
 231 GAN was deployed to ensure the realness of reenacted images,  
 232 moreover, we also applied GAN to make sure that landmark  
 233 coordinates generated by our method follows the distribution  
 234 of real landmark coordinates. Details of GAN in our method  
 235 are given in Section III.

### 236 III. METHOD

237 Figure 1 shows the overall framework of our face reenact-  
 238 ment model. In general, we first estimate an optical flow based  
 239 on input images. Then the eyes, nose and mouth in the source  
 240 image are individually reenacted. Lastly, we use the estimated

241 optical flow to warp the feature maps of the source image,  
 242 and use reenacted facial landmarks to guide the subsequent  
 243 image generation process. Specifically, when the identity of  
 244 the driving image is different from the source, we can no  
 245 longer leverage driving landmark coordinates for guidance  
 246 because of identity mismatch. We therefore estimate landmark  
 247 coordinates that match the source’s identity and the driver’s  
 248 expression and head pose. These landmark coordinates are  
 249 further adopted to yield style transfer parameters that improves  
 250 the quality of generated images, as shown in Figure 1(b).

#### 251 A. Optical Flow Estimation

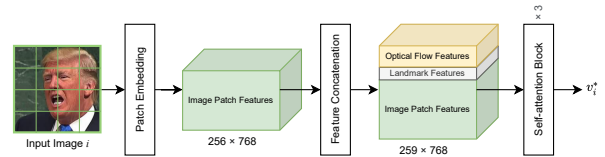


Fig. 2. Architecture of Vision Transformer as optical flow feature extractor.

252 Input images are sent to a neural network to extract features  
 253 for optical flow estimation. Considering the fact that face reen-  
 254 actment requires the information on expression over an entire  
 255 face, we adopt Vision Transformer as the feature extractor, as  
 256 Vision Transformer directly learns the attention over the entire  
 257 image while CNNs focus more on the locality of images. A  
 258 ResNet feature extractor is also evaluated in Section IV for  
 259 comparison.

260 For Vision Transformer in our method, its architecture is  
 261 shown in Figure 2. An input image  $i$  with size  $224 \times 224$   
 262 is divided into 256 patches with size  $14 \times 14$ . Each image  
 263 patch is embedded into a 768-dimensional vector, resulting in  
 264 a  $256 \times 768$  tensor  $v_i$  for an input image. In addition, a tensor  
 265  $t \in \mathbb{R}^{3 \times 768}$  with learnable initial values are concatenated  
 266 to  $v_i$ , the first two rows of  $t$  store features for the optical  
 267 flow estimation, and the third row of  $t$  contains features for  
 268 landmark coordinate regression, which acts as an auxiliary task  
 269 that helps the model perceive human faces. After an input

270 image being embedded into  $v_i \in \mathbb{R}^{259 \times 768}$ , it further goes  
 271 through three self-attention layers. The self-attention process  
 272 is given as follows.

$$Q = v_i W_q, K = v_i W_k, V = v_i W_v \quad (1)$$

$$\alpha = \text{softmax}(QK^T / \sqrt{d_k}), v_i^* = \alpha V \quad (2)$$

274 where  $W_q \in \mathbb{R}^{768 \times d_q}$ ,  $W_k \in \mathbb{R}^{768 \times d_k}$  and  $W_v \in \mathbb{R}^{768 \times d_v}$   
 275 are learn-able parameters, we set  $d_q = d_k = d_v = 768$ .  $\alpha \in$   
 276  $\mathbb{R}^{259 \times 259}$  is the attention score given the input tensor  $v_i$ , and  
 277  $v_i^* \in \mathbb{R}^{259 \times 768}$  is the output of the self-attention operation,  
 278 it further goes through an MLP layer to yield the final result  
 279 of a transformer block. Note that we only take the first two  
 280 rows of  $v_i^*$  as the feature for optical flow estimation. In the  
 281 case of ResNet, features obtained from the final global average  
 282 pooling layer are projected to the dimension of  $\mathbb{R}^{2 \times 768}$  that  
 283 matches Vision Transformer’s output.

284 Optical flow features for the source and the driving image  
 285 are denoted by  $u_s, u_d \in \mathbb{R}^{2 \times 768}$  respectively.  $u_s$  and  $u_d$  are  
 286 first compressed to  $\mathbb{R}^{2 \times 128}$  then reshaped to  $\mathbb{R}^{1 \times 256}$ , next,  
 287 these two features are concatenated and sent to an multi-  
 288 layer perceptron, resulting in  $f \in \mathbb{R}^{1 \times 6272}$ ,  $f$  is reshaped to  
 289  $\mathbb{R}^{7 \times 7 \times 128}$  and after going through a series of transpose con-  
 290 volutional layers, the estimated optical flow  $f^* \in \mathbb{R}^{2 \times 224 \times 224}$   
 291 is obtained.

### 292 B. Individual Landmark Reenactment

293 Our motivation for individually reenacting facial landmarks  
 294 is to help the model correctly perceive human faces when reen-  
 295 acting different identities. We observed that without explicitly  
 296 specifying individual facial landmarks in the image generator,  
 297 the model tends to synthesize more mouths or eyes than they  
 298 should be on a single face when the source and the driving  
 299 have different identities. This problem is more likely to happen  
 300 when the model is trained on a dataset with fewer identities,  
 301 such as CelebV. Another benefit of individually reenacting  
 302 facial landmarks is that these landmarks can be aligned based  
 303 on landmark coordinates to explicitly guide the reenactment  
 304 process. We use four convolutional neural networks with  
 305 an identical architecture, and each of them is dedicated to  
 306 reenacting a different part of the face, namely the left eye,  
 307 the right eye, the nose, and the mouth. Figure 3(a) shows we  
 308 concurrently reenact selected landmarks; Figure 3(b) gives an  
 309 example of the crop of the mouth from the source image,  
 310 along with its counterpart from the landmark heatmap of the  
 311 driving image are first sent to convolution layers, with the size  
 312 of feature maps reduced by max pooling, then feature maps  
 313 of the RGB mouth crop and that of the landmark heatmap are  
 314 added element-wise and sent to transpose convolution layers  
 315 to generate reenacted landmarks. All crops are fixed-sized and  
 316 they are cropped around the centre point of corresponding  
 317 landmark coordinates. The size of a landmark crop takes the  
 318 value of the average size of corresponding landmark in the  
 319 dataset. The landmark heatmap is obtained by first drawing  
 320 68 facial landmark points on a  $224 \times 224$  image with black  
 321 background, then points are connected by fitting B-spline

322 curves, drawing the outlines of the face, eyes, eye brows, nose  
 323 and mouth. When all landmarks are reenacted, they are directly  
 324 placed on another blank  $224 \times 224$  image  $I_p$ , and their centre  
 325 point all align with the centre point of corresponding parts in  
 326 the landmark heatmap.

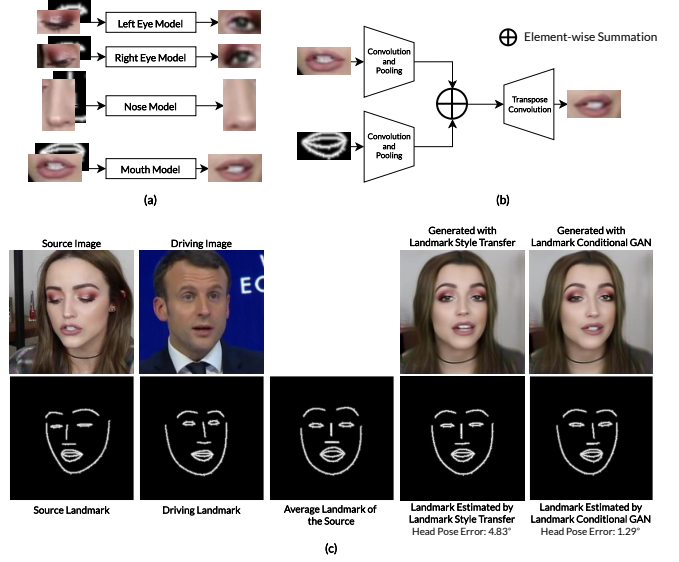


Fig. 3. (a) Individual landmarks are concurrently reenacted with models that share the same architecture. (b) Example of mouth reenactment showing the architecture of the landmark reenactment model. (c) Landmark coordinates estimated by style transfer significantly sacrifice head pose accuracy for identity preserving, whereas landmark conditional GAN better balances this trade off.

327 1) *Landmark Coordinate Style Transfer*: Since the driving  
 328 landmark coordinates need to be modified to fit the source’s  
 329 identity, and inspired by [33]; we first propose a naive method  
 330 for estimating the landmark coordinates, i.e., aligning the mean  
 331 and variance of the driving coordinates  $lmk_{driving}$  and those  
 332 of the source coordinates  $lmk_{source}$ . The alignment is defined as,  
 333

$$lmk_{reenact} = \frac{lmk_{driving} - \mu_{driving}}{\sigma_{driving}} \times \sigma_{source} + \mu_{source} \quad (3)$$

334  $\mu_{source}, \sigma_{source}, \mu_{driving}, \sigma_{driving}$  can be obtained by com-  
 335 puting the mean and variance of each person’s landmark  
 336 coordinates in the dataset, no learning is involved in this  
 337 process. We also shift  $lmk_{reenact}$  such that its centre point  
 338 is at the same location as  $lmk_{driving}$ . Figure 3(b) shows  
 339 an example the driving landmark heatmap generated by the  
 340 original landmark coordinates and the one generated by style-  
 341 transferred coordinates.

342 2) *Landmark Conditional GAN*: One major problem with  
 343 the above landmark style transfer is that Equation 3 pushes  
 344 landmark coordinates towards the average head pose in the  
 345 dataset instead of truthfully acting as the desired pose. As  
 346 shown in Figure 3(b), landmark coordinates modified by style  
 347 transfer To remedy this problem, we propose the landmark  
 348 conditional GAN as a more reliable estimator.

AU1	AU2	AU4	AU5	AU6	AU7
Inner Brow Raiser	Outer Brow Raiser	Brow Lowerer	Upper Lid Raiser	Cheek Raiser	Lid Tightener
AU9	AU10	AU12	AU14	AU15	AU17
Nose Wrinkler	Upper Lip Raiser	Lip Corner Puller	Dimpler	Lip Corner Depressor	Chin Raiser
AU20	AU23	AU25	AU26	AU28	AU45
Lip Stretcher	Lip Tightener	Lips Apart	Jaw Drop	Lip Suck	Blink

Fig. 4. Facial action units (AUs) in this study.

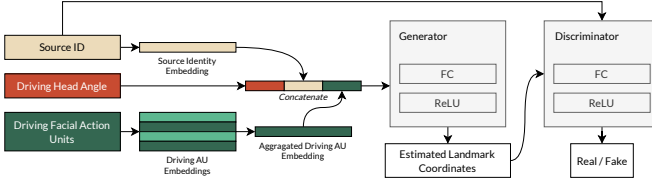


Fig. 5. The architecture of landmark conditional GAN.

The input to our conditional GAN is inspired by the evaluation metrics of face reenactment methods, specifically, we feed the source’s identity, the driving’s head pose, and facial action units appeared on the driving’s face into the generator to obtain 68 2-D landmark coordinates. Facial action units (AUs) are predefined basic muscle movements on human faces. Figure 4 shows selected AUs in our method, these AUs are also used for face reenactment evaluation.

The convention of AU study is that a complex expression can be expressed by the addition of many different facial action units. For instance, an unhappy mouth can be expressed as AU15+AU17. We then took a similar approach to process AUs in the conditional GAN. Embedding vectors of facial action units appeared in the driving image are first selected, then these vectors are summed up to yield the overall expression feature for the input. The overall architecture of landmark conditional GAN is shown in Figure 5.

### C. Image Generator

The face reenactment module is a U-Net-like convolutional neural network with only one skip-connection in the middle, Figure 5 shows its overall architecture. The source image is first sent to three convolutional layers with the size of its feature map  $r$  being reduced to  $58 \times 58$ , then the estimated optical flow map  $f^*$  (Section 2.1) with size  $224 \times 224$  is resized to match the size of  $r$  and warps  $r$ , yielding the warped feature map  $r^*$ . The image  $I_p$  with reenacted landmark parts from the landmark reenactment module (Section 2.2) is also resized to  $58 \times 58$  and concatenated to  $r^*$ . The concatenated feature map  $r_{cat}^*$  continues to go through intermediate convolutional layers with no change in feature map size, then  $r^*$  is concatenated to  $r_{cat}^*$  through the skip connection, the resulting feature map is further upsampled through bilinear interpolation and processed

by convolution layers to generate the final reenacted image. The use of bilinear upsampling is aiming for alleviating the checkerboard artifact in images generated by convolutional neural networks [36].

1) *Style Transfer Branch*: In the case of reenacting different identities, although our landmark estimation methods greatly alleviated the identity preserving problem, unnatural face deformations exist as a result of inaccurate optical flow estimation. To rectify this issue, we further introduce a style transfer branch to the generator. The architecture of the style transfer branch is inspired by StyleGAN2 [26]. Instead of estimating style transfer parameters from random inputs, our model takes 1-channel landmark heatmaps as input. These landmark heatmaps are generated by first estimating the landmark coordinates using the conditional GAN in Section III.B.(2), then b-spline curves are fitted between adjacent landmark points that belong to the same facial landmark, namely drawing out the contours of the face, eyes, eyebrows, nose, and mouth. The use of heatmaps avoids the identity leak which is destined to happen if RGB driving images were used. Furthermore, since the heatmaps are generated based on coordinates estimated by our landmark conditional GAN, the identity information of the driving person is excluded as much as possible. The architecture of the style transfer branch is show in Figure 5.

### D. Loss Function

Overall we use the weighted sum of four types of loss function to train our face reenactment model.

- L1 Loss: L1 loss is responsible for supervising the pixel value in generated images. During training, driving images are also the groundtruths for generated images, L1 loss is computed between these images. The weight on this loss is set to 20 for the entire image, and 5 for individually reenacted landmarks. We find that putting more weight on the L1 loss prevents the model from generating unexpected artifacts.
- Adversarial Loss: The adversarial loss we used for training is the same as [28]. Driving images are treated as "real samples" while reenacted images are labeled as "fake". We set the weight for this loss to 1.
- GAN Feature Matching Loss [27]: GAN feature matching requires the discriminator to return intermediate features of real and generative samples, then forcing these features to be the same. For generative tasks with groundtruth samples, GAN feature matching loss makes the training more stable and converge faster. The weight for this loss is set to 1.
- Perceptual Loss [29]: Perceptual loss relies on a pre-trained VGG model to extract shallow visual features for real and generative samples. Pushing these features to be close ensures that low level features in the generated image, such as the shape of the face and shoulder, to be more realistic. The weight for this loss is set to 10.

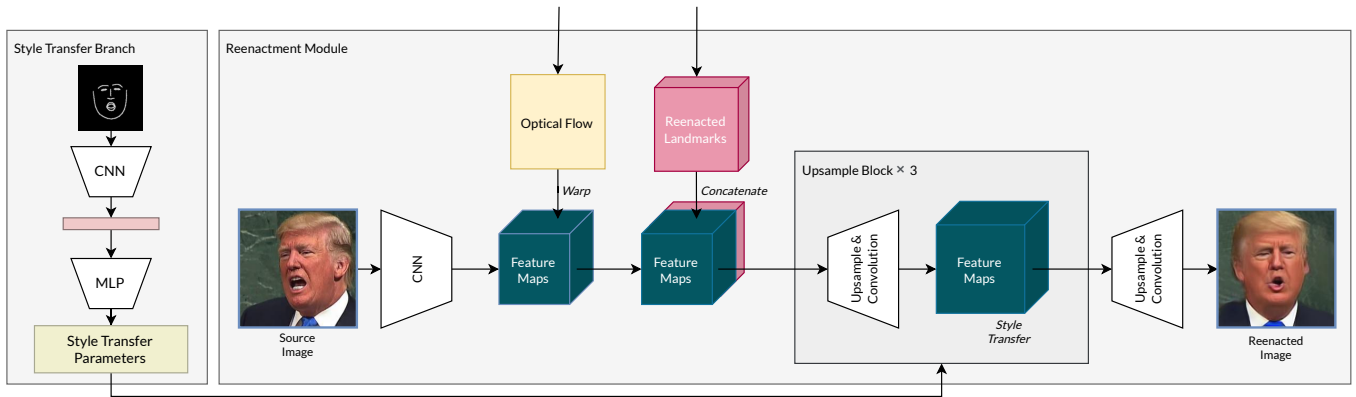


Fig. 6. The style transfer branch and the image generator.

#### IV. EXPERIMENTS

##### A. Datasets and Experimental Settings

We evaluated our methods on the VoxCeleb1 dataset for self-reenactment, and the CelebV dataset for reenacting different identities. VoxCeleb1 is a dataset with 22,496 video clips extracted from YouTube. It contains 1,251 identities, and people’s faces have been cropped into  $256 \times 256$  images. CelebV has around 40,000 images for each of the five people in the dataset. For each person, their images are sampled from the same video and has also been cropped into  $256 \times 256$  images.

For self-reenactment, we followed the protocol in [7], [11] and trained our model on the VoxCeleb1 dataset. The test set for evaluation consists of 100 videos from the test split given by the authors of VoxCeleb1, 2,083 source-driving image pairs are sampled from these videos for evaluation. For reenacting different identities, since our landmark conditional GAN and style transfer module require the information of known identities, we evaluated our method in two different scenarios. The first scenario follows [7], [11] and aims at reenacting unseen identities. Models are only trained on the VoxCeleb1 dataset, however, the test set are image pairs sampled from the CelebV dataset. For each person in CelebV, 2,000 source-driving image pairs are randomly sampled. In the second scenario, models are only trained on the CelebV dataset. Test set in this case also comprises 2,000 source-driving image pairs randomly sampled for each person.

##### B. Model Variants

We evaluated two model variants, denoted by their backbone network for optical flow estimation, namely ViT and ResNet. Further ablation studies were also conducted to validate the proposed landmark GAN and style transfer branch. The ViT model has three Vision Transformer layers for optical flow estimation, for the ResNet variant, transformer layers are replaced by ResNet-34. In the work of [22], a modified ResNet-50 (25 million parameters) outperforms the base 12-layer Vision Transformer (86 million parameters) on ImageNet top-1 accuracy by 10% with a pre-training dataset of 10M images.

Given that there are three Vision Transformer layers (19M parameters) in our baseline model, we hence choose ResNet-34 (21M parameters) for comparison, which is shallower than ResNet-50. Additionally, we applied landmark style transfer described in Section 2.2 to both models and evaluated their performance accordingly. Models with landmark style transfer are denoted by ViT+LSt and ResNet-34+LSt.

##### C. Metrics

Performance on self-reenactment was evaluated through the following metrics, cosine similarity (CSIM), structural similarity (SSIM), peak signal-to-noise ratio (PSNR), root mean square error of head pose angles (PRMSE), and the ratio of correct facial action units (AUCON). CSIM measures the model’s capability on identity preserving. It is derived from the cosine similarity between embedding vectors of the source and generated image, these vectors are extracted by a pretrained face recognition model Arcface [32]. SSIM and PSNR are exclusive to self-reenactment evaluation as they both require ground-truth images to compute, which is not possible for reenacting different identities. PSNR evaluates low-level similarity between generated images and ground-truths, while SSIM jointly evaluates the contrast, luminance, and structural between images. Head pose angles and facial action units are detected by OpenFace [30]. PRMSE is computed by calculating the root mean square error of head pose angles of the generated image compared against those of the driving image. For AUCON, both the driving and generated image are sent to OpenFace, the returned results show if facial action units in Figure 4 appear or not in the given image. Given the AU recognition results of the driving image, the ratio of AUs that correctly appear or do not appear in the generated image yields the AUCON.

##### D. Experimental Results and Analysis

Our experiments show that landmark coordinates of the driving image is a helpful heuristics for preserving the source’s identity and achieving accurate head poses. By directly using driving landmark coordinates to guide the alignment of individual landmarks in the generated image, our model achieved

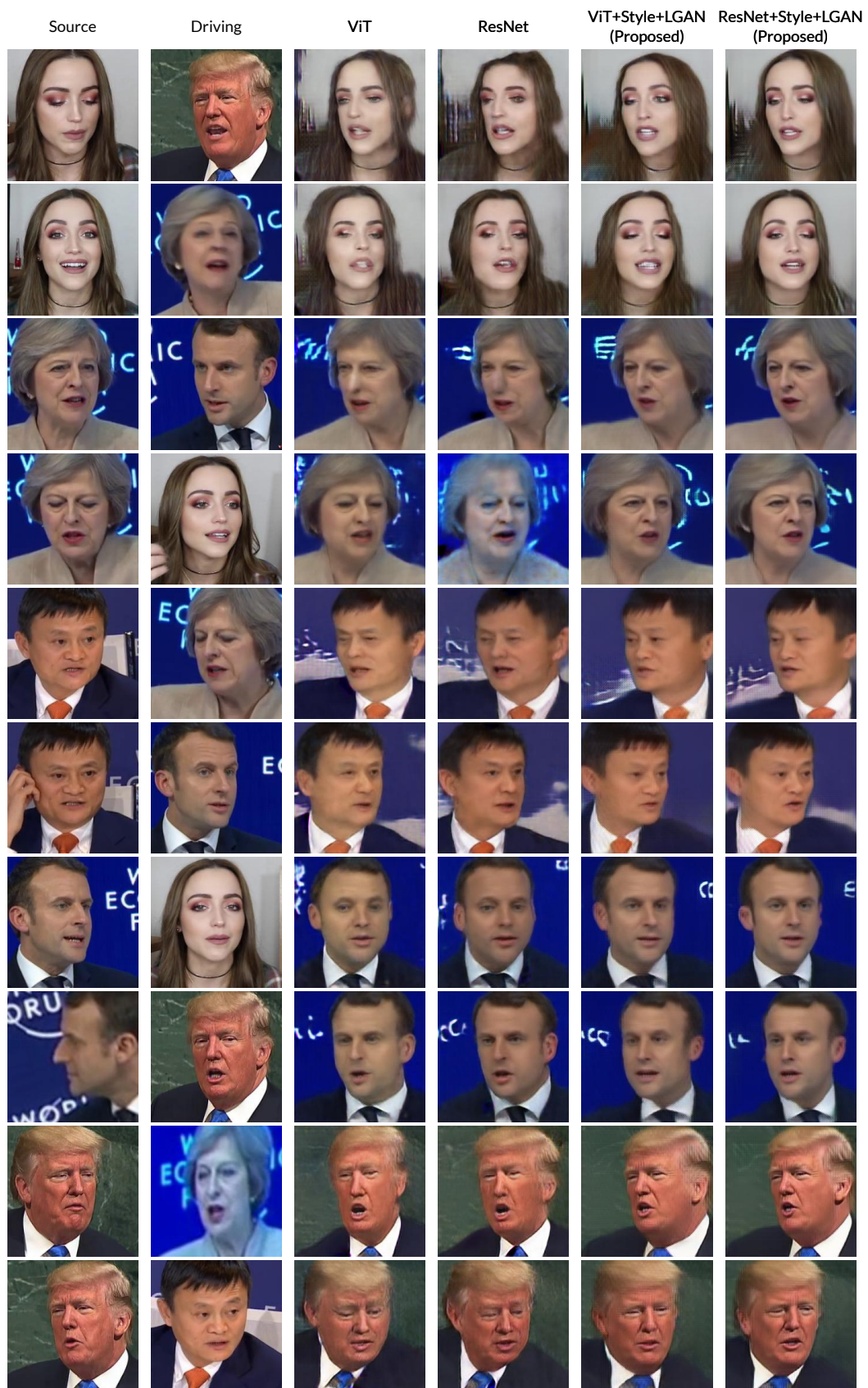


Fig. 7. Qualitative results of proposed models on CelebV dataset.

TABLE I  
EVALUATION OF SELF-REENACTMENT ON VOXCELEB1

Model	CSIM $\uparrow$	SSIM $\uparrow$	PSNR $\uparrow$	PRMSE $\downarrow$	AUCON $\uparrow$
Mesh Guided GCN [11]	0.822	<u>0.739</u>	<b>30.394</b>	3.20	<b>0.887</b>
MarioNETte [7]	0.755	<b>0.744</b>	23.244	3.13	0.825
Monkey-Net [9]	0.697	0.734	23.472	3.46	0.770
FirstOrder [8]	0.813	0.723	<u>30.182</u>	3.79	<u>0.886</u>
NeuralHead-FF [31]	0.229	0.635	20.818	3.76	0.791
X2face [6]	0.689	0.719	22.537	3.26	0.813
ViT	<b>0.879</b>	0.608	29.297	<u>1.97</u>	0.767
ResNet	0.878	0.650	29.606	<b>1.58</b>	0.793

**Bold** shows the best results, second bests are underlined.  $\uparrow$  indicates the larger the value, the better the performance,  $\downarrow$  means otherwise.

TABLE II  
EVALUATION OF REENACTING DIFFERENT IDENTITIES WITH UNSEEN DATA ON CELEBV

Model	CSIM $\uparrow$	PRMSE $\downarrow$	AUCON $\uparrow$
MarioNETte [7]	0.520	3.41	0.710
Mesh Guided GCN [11]	<b>0.635</b>	3.41	0.709
Monkey-Net [9]	0.451	4.81	0.584
FirstOrder [8]	0.462	3.90	0.667
NeuralHead-FF [31]	0.108	3.30	<b>0.722</b>
X2face [6]	0.450	3.62	0.679
ViT	0.525	2.95	0.694
ResNet	0.515	<b>2.35</b>	0.708

TABLE III  
EVALUATION OF REENACTING DIFFERENT IDENTITIES WITH MODELS TRAINED ON CELEBV

Model	CSIM $\uparrow$	PRMSE $\downarrow$	AUCON $\uparrow$
X2Face [6]	0.467	8.12	0.611
ViT	0.568	2.77	0.692
ViT+LGAN+Style	<u>0.653</u>	<u>2.66</u>	0.675
ResNet	0.570	<b>2.57</b>	<b>0.695</b>
ResNet+LGAN+Style	<b>0.661</b>	2.68	0.672

TABLE IV  
EVALUATION OF LANDMARK ESTIMATION FOR REENACTING DIFFERENT IDENTITIES ON CELEBV

Model	CSIM $\uparrow$	PRMSE $\downarrow$	AUCON $\uparrow$
ViT	0.568	2.77	<u>0.692</u>
ViT+LSt	<b>0.620</b>	3.87	0.646
ViT+LGAN	0.619	2.60	0.682
ResNet	0.570	<u>2.57</u>	<b>0.695</b>
ResNet+LSt	0.616	3.78	0.650
ResNet+LGAN	0.614	<b>2.49</b>	0.687

TABLE V  
EVALUATION OF STYLE TRANSFER FOR REENACTING DIFFERENT IDENTITIES ON CELEBV

Model	CSIM $\uparrow$	PRMSE $\downarrow$	AUCON $\uparrow$
Style	<b>0.647</b>	4.75	0.646
ViT	0.568	<u>2.77</u>	<u>0.692</u>
ViT+Style	0.587	3.22	0.668
ResNet	0.570	<b>2.57</b>	<b>0.695</b>
ResNet+Style	<u>0.606</u>	2.97	0.670

510 better performance on identity preserving and head pose  
511 accuracy on the VoxCeleb1 dataset, shown in Table I.

512 Following evaluation protocols in [7], [11], we evaluate our  
513 baseline models trained on VoxCeleb1 for reenacting unseen  
514 people from the CelebV test set. Shown in Table II, our  
515 methods still have lower head pose error, however, the identity  
516 preserving capability is less ideal compared to Mesh Guided  
517 GCN [11]. The main reason is that the driving’s identity  
518 information was dismissed in the optical flow estimation stage  
519 of [11]. The landmark GAN and style transfer module we  
520 proposed are aiming at alleviating the identity preserving  
521 problem. These methods are designed to leverage training  
522 data to improve the quality of generated images, hence their  
523 evaluation are shown in separate tables, viz. Table III. In  
524 general, both landmark GAN and style transfer can improve  
525 the model’s identity preserving capability. When combined  
526 together, our method achieves better identity preserving ca-  
527 pability while maintaining a lower head pose error.

528 1) *Self-reenactment*: Table I shows models’ performance  
529 on the VoxCeleb1 dataset. Our method better preserves iden-  
530 tities (higher CSIM) and shows lower error on head pose  
531 angles (lower PRMSE). This illustrates that coordinates of  
532 driving landmarks are a strong prior that can help models

533 perform better on these two metrics. SSIM takes the structural  
534 similarities into consideration, which includes both the face  
535 and background of the image. Our method pays more attention  
536 on the face region, backgrounds in reenacted images are often  
537 distorted, resulting in a low score in SSIM. We believe the  
538 expression accuracy (AUCON) of our method is related to  
539 the presumption made in terms of reenacting individual facial  
540 landmarks. In the preprocessing stage, eyes and mouths for all  
541 people in the dataset are cropped into fixed sizes to ensure that  
542 the landmark reenactment model can handle varying landmark  
543 and camera movement in images. However, this also limits  
544 the model’s capability as there are cases where landmarks  
545 cannot fit in the cropped region. For instance, a wide open  
546 mouth or a close-up camera can lead to a larger mouth region,  
547 the model may still try to fit the entire mouth into region  
548 we cropped, resulting in less accurate expression reenactment.  
549 This phenomenon is also observed when reenacting different  
550 identities.

551 2) *Reenacting Different Identities*: Table II shows the over-  
552 all performance on the CelebV dataset for models trained only  
553 on the VoxCeleb1 dataset. As mentioned above, Mesh Guided  
554 GCN [11] excluded the driving’s identity when reconstructing  
555 3D face models, the optical flows are then estimated based  
556 on these 3D models, leading to better identity preserving in

557 generated images. With the guidance of landmark locations,  
558 our methods show more accurate head poses, since these  
559 landmark locations do not reflect the identity of the source  
560 image, our methods performs poorer than the self-reenactment  
561 scenario. In Figure 8, we cited image from [7] to compare  
562 images generated by different models.

563 The proposed landmark estimation and style transfer meth-  
564 ods rely on learning from training samples to assist the image  
565 generation process, we then trained these models on the  
566 CelebV dataset. X2Face [6] is also trained from scratch on  
567 CelebV for comparison. Shown in Table III, X2Face shows  
568 slightly better identity preserving compared to results in Table  
569 II, however, the head pose error significantly increased. We  
570 found that X2Face has difficulty in converging when trained  
571 on a smaller dataset such as CelebV. Our methods achieve  
572 better identity preserving and lower head pose error thanks to  
573 the proposed landmark GAN and style transfer module.

574 3) *ViT vs ResNet*: In general, the ResNet variant of our  
575 method performs slightly better than its ViT counterpart. We  
576 believe this is because estimated optical flows are used to warp  
577 CNN features regardless of the network’s backbone. ResNet  
578 is more compatible with this feature representation as it is  
579 also a CNN based model. However, Vision Transformer is still  
580 promising for face reenactment. When evaluated on ImageNet  
581 [22] with 10 million images for training, a Vision Transformer  
582 with 86 million parameters is outperformed by ResNet-50  
583 with only 25 million parameters. In our case, the ViT head  
584 for optical flow estimation has 19 million parameters while  
585 the ResNet head has 21 million parameters. Our results show  
586 that the performance difference between these two models is  
587 negligible, a future study on Vision Transformer based image  
588 generator for face reenactment is worth investigating.

589 4) *Landmark Estimation and Style Transfer*: Table IV  
590 shows the ablation study on proposed landmark estimation  
591 methods. Landmark Style Transfer, denoted by LSt, is a  
592 crude way of estimating landmark coordinates, it achieves  
593 the best identity preserving among evaluated models, but it  
594 also significantly hinders the pose and expression accuracy.  
595 Landmark conditional GAN (LGAN), on the other hand, better  
596 balances these metrics.

597 Table V shows the ablation study on style transfer. The  
598 model named "Style" is a baseline model without optical flow  
599 estimation, its reenactment process solely relies on the image  
600 generator and style transfer branch in Figure 6. Although this  
601 model shows relatively good identity preserving capability, it  
602 generates images with the poorest quality. Facial textures in  
603 generated images are often a mixture of the source and driving  
604 image. Although we explicitly excluded the RGB information  
605 from the style transfer input by using one-channel landmark  
606 heatmaps instead, the model "memorizes" the connection  
607 between landmark heatmaps and their corresponding color  
608 images due to the self-supervised nature of the training stage.  
609 Evaluation metrics also show that style transfer promotes our  
610 models’ the identity preserving capability at the cost of head  
611 pose and expression accuracy. However, this does not reflect  
612 the real contribution of style transfer. As shown in Figure 9,

613 faces generated by non-style-transfer methods are distorted  
614 because of the warp operation, style transfer can help our  
615 model revert unnecessary distortion on faces, generating more  
616 realistic images.

617 5) *Comparison with FSGANv2*: Unlike most methods in  
618 Table I, the face reenactment of FSGANv2 does not rely on  
619 the optical-flow-based warping operation to generate images.  
620 We cited generated images from [37] to compare FSGANv2  
621 with our method. Figure 10 shows the comparison between our  
622 ViT model and FSGANv2 on self-reenactment. The image at  
623 the top left corner is served as the the source image, while all  
624 images in the first row are driving images. In this scenario,  
625 when the difference between head pose angles are relatively  
626 small, both methods can generate realistic faces, while our  
627 method preserves sharper details in the source’s face. As the  
628 head pose angles increase, the quality of generated images  
629 decreases for both methods. Figure 11 shows the comparison  
630 on reenacting different identities. Both the source and driving  
631 images are in-the-wild samples for our model. In addition,  
632 our landmark GAN and the style transfer branch is limited  
633 to working on known faces, therefore we also opted to the  
634 ViT model in Table I for this comparison. As mentioned in  
635 Section I, FSGANv2 iteratively rotates facial landmarks then  
636 synthesizes images based on rotated landmark points, enabling  
637 FSGANv2 to better preserve facial structures in generated  
638 images.

## 639 V. CONCLUSIONS AND FUTURE WORK

640 We propose a face reenactment method guided by gener-  
641 ative landmark coordinates. We evaluated our method in the  
642 following scenarios:

- 643 • **Self-reenactment.** In this scenario, the source and the  
644 driving image are taken from the same video clip of the  
645 same person, which allows us to directly use landmark  
646 coordinates in the driving image to guide the reenactment.  
647 We evaluated our method on the VoxCeleb1 dataset and  
648 compared against exiting methods following the same  
649 protocol. We show that images generated by our method  
650 are more similar to the input image’s identity, and our  
651 method has lower head pose error compared to others.  
652 Our result show that landmark coordinates in the driving  
653 image are informative and helpful for identity preserving  
654 and accurately reenacting head pose angles.
- 655 • **Reenacting Different Unknown Identities.** In this sce-  
656 nario, the identities of the source and the driving image  
657 are different and they are not included in the training  
658 set. We used our self-reenactment model trained on Vox-  
659 Celeb1 for evaluation on the CelebV dataset. Our method  
660 still managed to achieve lower head errors, indicating that  
661 the heuristic of using driving landmark coordinates to  
662 guide face reenactment is beneficial for accurately reen-  
663 acting head movement. However, landmark coordinates  
664 require further adjustment to match the source face’s  
665 identity.
- 666 • **Reenacting Different Known Identities.** In this sce-  
667 nario, the identities of the source and the driving image

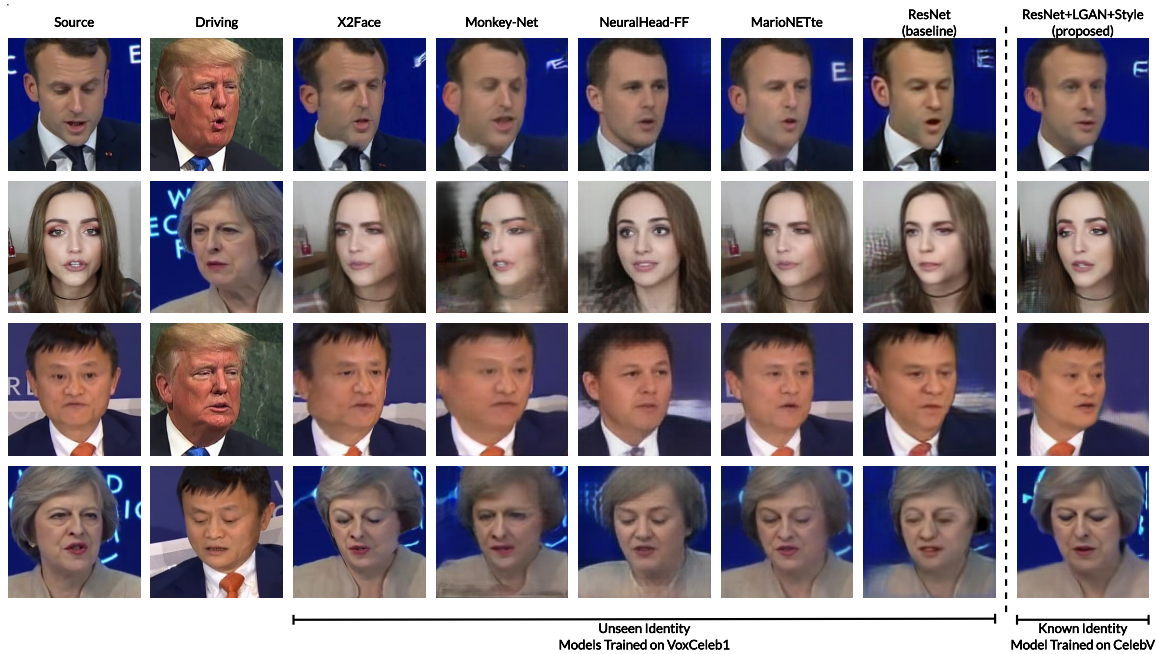


Fig. 8. Comparison of Reenacting Different Identities on CelebV.



Fig. 9. Optical flow combined with style transfer improved the quality of generated images.



Fig. 11. Comparison with FSGANv2 on Reenacting Different Identities.



Fig. 10. Comparison with FSGANv2 on Self-reenactment

transfer branch fixes shape distortions in generated images. When these two modules are combined together, the performance on identity preserving is greatly improved while the head pose errors remain relatively low. This proves that using head pose angles and facial action units can effectively estimate landmark coordinates of desired faces.

One noticeable limitation of our method is that it does not generate well to reenacting different and unknown identities. Our method heavily relies on landmark coordinates, but proposed landmark estimation method is only applicable to known faces. Another limitation of our method involves the proposed style transfer branch. Because the input to this

668 are different but they all appear in the training set. We  
 669 proposed the landmark conditional GAN and the style  
 670 transfer branch to assist our baseline model. Ablation  
 671 experiments show that the landmark conditional GAN  
 672 mainly contributes to identity preserving while the style

673  
 674  
 675  
 676  
 677  
 678  
 679  
 680  
 681  
 682  
 683  
 684  
 685

686 module is a facial landmark heatmap, the modules struggles  
687 with appearance variations in the training data. For instance,  
688 in the VoxCeleb1 dataset, there are multiple video clips for  
689 the same person. The person may have beard in one video but  
690 the beard may be shaved in another video. In this case, the  
691 style transfer branch tends to remove the beard in generated  
692 images because the beard is not represented in the input.

693 Based on the above limitations, we suggest that one possible  
694 future work is to enhance the proposed landmark estimation  
695 method’s generalisation capability. More generalised identity  
696 representations, such as identity embeddings from a face  
697 recognition model, can be used. Another topic worth in-  
698 vestigating is to develop the style transfer branch that can  
699 handle varying appearances. Instead of modifying the entire  
700 feature maps, we could only transfer the styles to facial  
701 regions that needs changing. Lastly, we argue that it is also  
702 possible to design Vision Transformer based image generator.  
703 The performance of our model with the Vision Transformer  
704 backbone is lower than its ResNet counterpart. We believe  
705 this is because our estimated optical flows are used to warp  
706 feature maps estimated by a CNN, therefore ResNet is more  
707 compatible with this task. A Vision Transformer based image  
708 generator may be more suitable to the Vision Transformer  
709 backbone, however, how to define the warping operation on  
710 intermediate features of the Vision Transformer is still an open  
711 problem.

## 712 REFERENCES

713 [1] J. Thies, M. Zollhöfer, M. Stamminger, C. Theobalt, and M. Nießner,  
714 “Face2face: Real-time face capture and reenactment of rgb videos,” in  
715 CVPR 2016.  
716 [2] Y.-T. Cheng, et al., “3D-model-based face replacement in video,” in  
717 SIGGRAPH, 2009.  
718 [3] H. Kim, et al., “Deep video portraits,” in ACM Transactions on Graphics,  
719 2018.  
720 [4] S. Suwajanakorn, S. M. Seitz, and I. Kemelmacher-Shlizerman, “What  
721 makes tom hanks look like tom hanks,” in ICCV, 2015.  
722 [5] D. Vlastic, M. Brand, H. Pfister, and J. Popović, “Face transfer with  
723 multilinear models,” ACM Trans. Graph., 2005.  
724 [6] O. Wiles, A. S. Koepke, and A. Zisserman, “X2face: A network for  
725 controlling face generation using images, audio, and pose codes,” in  
726 ECCV, 2018  
727 [7] S. Ha, M. Kersner, B. Kim, S. Seo, and D. Kim, “Marionette: Few-shot  
728 face reenactment preserving identity of unseen targets,” in AAAI, 2020.  
729 [8] A. Siarohin, S. Lathuilière, S. Tulyakov, E. Ricci, and N. Sebe, “First  
730 order motion model for image animation,” in Advances in Neural  
731 Information Processing Systems, 2019  
732 [9] A. Siarohin, S. Lathuilière, S. Tulyakov, E. Ricci, and N. Sebe,  
733 “Animating arbitrary objects via deep motion transfer,” in CVPR, 2019  
734 [10] G. Yao, Y. Yuan, T. Shao, S. Li, S. Liu, Y. Liu, M. Wang, and K. Zhou,  
735 “One-shot face reenactment using appearance adaptive normalization,”  
736 in AAAI, 2021  
737 [11] G. Yao, Y. Yuan, T. Shao, and K. Zhou, “Mesh guided one-shot  
738 face reenactment using graph convolutional networks,” in 28th ACM  
739 International Conference on Multimedia, 2020.  
740 [12] X. Zeng, Y. Pan, M. Wang, J. Zhang, and Y. Liu, “Realistic face  
741 reenactment via self-supervised disentangling of identity and pose,” in  
742 AAAI, 2020.  
743 [13] M. Jaderberg, K. Simonyan, A. Zisserman, and k. kavukcuoglu, “Spatial  
744 transformer networks,” in NIPS, 2015.  
745 [14] V. Blanz and T. Vetter, “A morphable model for the synthesis of 3d  
746 faces,” in SIG-GRAPH, 1999.  
747 [15] A. Ranjan, T. Bolkart, S. Sanyal, and M. J. Black, “Generating 3D faces  
748 using convolutional mesh autoencoders,” in ECCV, 2018.

[16] W. V. F. Ekman, P., “The facial action coding system: A technique for  
749 measurement of facial movement,” 1978. 750  
[17] I. Goodfellow, J. Pouget-Abadie, M. Mirza, B. Xu, D. Warde-Farley,  
751 S. Ozair, A. Courville, and Y. Bengio, “Generative adversarial nets,” in  
752 NIPS, 2014. 753  
[18] M. Mirza and S. Osindero, “Conditional generative adversarial nets,” in  
754 arxiv: 1411.1784, 2014. 755  
[19] S. Reed, Z. Akata, X. Yan, L. Logeswaran, B. Schiele, and H. Lee,  
756 “Generative adversarial text to image synthesis,” in ICML, 2016. 757  
[20] P. Isola, J.-Y. Zhu, T. Zhou, and A. A. Efros, “Image-to-image translation  
758 with conditional adversarial networks,” in CVPR, 2017. 759  
[21] T.-C. Wang, M.-Y. Liu, J.-Y. Zhu, G. Liu, A. Tao, J. Kautz, and B.  
760 Catanzaro, “Video-to-video synthesis,” in NeurIPS, 2018. 761  
[22] A. Dosovitskiy, et al., “An image is worth 16x16 words: Transformers  
762 for image recognition at scale,” in ICLR, 2021. 763  
[23] A. Vaswani, N. Shazeer, N. Parmar, J. Uszkoreit, L. Jones, A. N. Gomez,  
764 L. u. Kaiser, and I. Polosukhin, “Attention is all you need,” in NIPS,  
765 2017. 766  
[24] Y. Liu, Y. Zhang, Y. Wang, F. Hou, J. Yuan, J. Tian, Y. Zhang, Z. Shi, J.  
767 Fan, and Z. He, “A survey of visual transformers,” in arXiv: 2111.06091,  
768 2021. 769  
[25] F. Zhu, Y. Zhu, L. Zhang, C. Wu, Y. Fu, and M. Li, “A unified efficient  
770 pyramid transformer for semantic segmentation,” in ICCV Workshops,  
771 2021. 772  
[26] T. Karras, S. Laine, M. Aittala, J. Hellsten, J. Lehtinen, and T. Aila,  
773 “Analyzing and improving the image quality of stylegan,” in CVPR,  
774 2020. 775  
[27] Wang, T.C., Liu, M.Y., Zhu, J.Y., Tao, A., Kautz, J., Catanzaro, B.,  
776 “High- resolution image synthesis and semantic manipulation with  
777 conditional gans,” in CVPR, 2018 778  
[28] Radford, A., Metz, L., Chintala, S., “Unsupervised representation learning  
779 with deep convolutional generative adversarial networks,” in ICLR,  
780 2016 781  
[29] Johnson, J., Alahi, A., Fei-Fei, L., “Perceptual losses for real-time style  
782 transfer and super-resolution,” in EVVC 2016 783  
[30] Baltrusaitis, T., Zadeh, A., Lim, Y.C., Morency, L.P., “Openface 2.0:  
784 Facial behavior analysis toolkit,” in 13th IEEE International Conference  
785 on Automatic Face Gesture Recognition, 2018 786  
[31] Zakharov, E., Shysheya, A., Burkov, E., Lempitsky, V., “Few-shot  
787 adversarial learning of realistic neural talking head models,” in ICCV,  
788 2019 789  
[32] Deng, J., Guo, J., Xue, N., Zafeiriou, S., “Arcface: Additive angular  
790 margin loss for deep face recognition,” in CVPR, 2019 791  
[33] Huang, X., Belongie, S., “Arbitrary style transfer in real-time with  
792 adaptive instance normalization,” in ICCV, 2017 793  
[34] Nagrani, A., Chung, J., Xie, W., Zisserman, A., “Voxceleb: Large-scale  
794 speaker verification in the wild,” in Computer Science and Language,  
795 2019 796  
[35] Wu, W., Zhang, Y., Li, C., Qian, C., Loy, C., “ReenactGAN: Learning  
797 to reenact faces via boundary transfer,” in EVVC 2018 798  
[36] Odena, A., Dumoulin, V., Olah, C., “Deconvolution and checkerboard  
799 artifacts,” in Distill 2016 800  
[37] Nirkin, Y., Keller, Y., Hassner, Tal, “FSGANv2: Improved Subject  
801 Agnostic Face Swapping and Reenactment,” in PAMI, 2022 802  
[38] Sun P., Li Y., Qi H., Lyu S., “LandmarkGAN: Synthesizing faces from  
803 landmarks,” in Pattern Recognition Letters, 2022 804